AAV-mediated Gene Therapy Halts Retinal Degeneration in PDE6β-deficient Dogs

Virginie Pichard[1], Nathalie Provost[1], Alexandra Mendes-Madeira[1], Lyse Libeau[1], Philippe Hulin[2], Kizito-Tshitoko Tshilenge[1], Marine Biget[1], Baptiste Ameline[1], Jack-Yves Deschamps[3], Michel Weber[4], Guylène Le Meur[4], Marie-Anne Colle[5], Philippe Moullier[1,6] and Fabienne Rolling[1]

[1]Atlantic Gene Therapies, INSERM UMR 1089, Université de Nantes, CHU de Nantes, Nantes, France; [2]Cellular and Tissular Imaging Core Facility of Nantes University, SFR Santé Francois Bonamy, INSERM UMS016/CNRS UMS3556, Nantes, France; [3]Emergency and Critical Care Unit, ONIRIS, Nantes-Atlantic College of Veterinary Medicine, Food Science and Engineering, Nantes, France; [4]CHU de Nantes, Service d'Ophtalmologie, Nantes, France; [5]UMR 703 PAnTher INRA/ONIRIS, Nantes-Atlantic College of Veterinary Medicine, Food Science and Engineering, Nantes, France; [6]Department of Molecular Genetics and Microbiology, College of Medicine, University of Florida, Gainesville, Florida, USA

We previously reported that subretinal injection of AAV2/5 RK.cpde6β allowed long-term preservation of photoreceptor function and vision in the rod-cone dysplasia type 1 (rcd1) dog, a large animal model of naturally occurring PDE6β deficiency. The present study builds on these earlier findings to provide a detailed assessment of the long-term effects of gene therapy on the spatio-temporal pattern of retinal degeneration in rcd1 dogs treated at 20 days of age. We analyzed the density distribution of the retinal layers and of particular photoreceptor cells in 3.5-year-old treated and untreated rcd1 dogs. Whereas no rods were observed outside the bleb or in untreated eyes, gene transfer halted rod degeneration in all vector-exposed regions. Moreover, while gene therapy resulted in the preservation of cones, glial cells and both the inner nuclear and ganglion cell layers, no cells remained in vector-unexposed retinas, except in the visual streak. Finally, the retinal structure of treated 3.5-year-old rcd1 dogs was identical to that of unaffected 4-month-old rcd1 dogs, indicating near complete preservation. Our findings indicate that gene therapy arrests the degenerative process even if intervention is initiated after the onset of photoreceptor degeneration, and point to significant potential of this therapeutic approach in future clinical trials.

Received 17 November 2015; accepted 2 February 2016; advance online publication 1 March 2016. doi:10.1038/mt.2016.37

INTRODUCTION

Retinitis pigmentosa (RP), or rod-cone dystrophy, is a rare and incurable hereditary retinal dystrophy that causes the sequential degeneration of rod and cone photoreceptors.[1] The first signs of RP include night blindness and the loss of peripheral vision due to progressive degeneration of rod photoreceptors.[2,3] Cone death occurs in the later stages of RP, resulting in the progressive loss of central vision. RP is characterized by genetic heterogeneity and affects approximately 1.5 million people worldwide. Of the more than 70 genes implicated in the etiology of RP to date, a mutation in the gene encoding the β subunit of rod cGMP-phosphodiesterase 6 (PDE6β) has been associated with one of the most prevalent forms of the disease, which accounts for ~1–2% of all human RP cases.[4–6] Only a few clinical patterns have been described for RP associated with the PDE6β mutation. Affected patients develop early-onset night blindness with progressive loss of the visual field.[7] By the age of 40, patients present the ophthalmologic hallmarks of RP: attenuated retinal vessels, waxy-looking optic nerve heads, pigmentary changes in the mid- and far-peripheral retina, and atrophic maculopathy, in some cases with central remnants of normal retinal pigmented epithelium (RPE).[8] Although some preservation of photopic responses may be observed, electroretinograms (ERGs) often fail to detect electrical activity.[9] Optical coherence tomography (OCT) in patients carrying the null mutation in the β-subunit of PDE6 has also revealed massive photoreceptor loss and abnormal laminar architecture.[10]

Currently, there is no effective treatment for RP caused by PDE6β deficiency. Initial attempts at gene therapy using various viral vectors including adenovirus, adeno-associated virus (AAV), and lentiviral vectors were tested in several murine models carrying different mutations in the *PDE6β* gene.[11–16] However, none of these first approaches resulted in sustained long-term functional rescue in a murine model of PDE6β deficiency, including rd1 and rd10 mice. A major limitation of these models is the massive and rapid photoreceptor degeneration that occurs; this leaves a narrow therapeutic window during which sufficient levels of transgene expression must be established in photoreceptors before the effects of degeneration become irreversible. However, thanks to significant advances in retinal gene therapy and an improved understanding of murine models, promising results have been reported in recent years with PDE6β-RP gene addition therapy.[17,18] Subretinal injection of 9×10^{10} viral genome (vg) of AAV 2/8 (Y733F)-SmCBA-mPDE6β in rd10 mice at postnatal day 14 has been shown to result in a 58% preservation of rod ERG responses and long-term morphological rescue.[17] More recently, Nishiguchi *et al.*[18] demonstrated that removal of a mutation in the *Gpr179* gene allows full restoration of vision in rd1 mice, the

Correspondence: Virginie Pichard, Atlantic Gene Therapies, INSERM UMR 1089, Institut de Recherche en Santé 1, Université de Nantes, 8 Quai Moncousu, 44007 Nantes Cedex 01, France. E-mail: virginie.pichard@univ-nantes.fr

most widely studied model of RP. Injections of 3×10^{10} vg of either AAV8 or AAV9 hRho.hPDE6β in rd1 mice lacking the *Gpr179* gene mutation result in the preservation of rows of photoreceptor nuclei (corresponding to 80% of that seen in wild-type controls), long-term rescue of ERG responses (approximately 60% with respect to wild-type controls) for up to 13 months postinjection, and vision-guided behavior that is absent in untreated animals.[18] Although murine models provide proof-of-concept, they have some limitations for the study of the specific long-term effects of gene therapy in PDE6β-RP. The low density of cones, particularly in the central area, makes the rodent retina an imperfect model for mimicking the PDE6β-RP phenotype, particularly the long-term preservation of cones in the fovea of patients with severe progressive rod-cone dystrophies. In the present study, we used the rcd1 dog, the eye of which is similar in size, anatomy, and retinal structure to the human eye. One of the most relevant homologies is photoreceptor distribution, particularly the cone-enriched region analogous to the macula[19] (the visual streak). The rcd1 dog, which mimics the severe rod-cone dystrophy observed in humans, carries a (2420G>A) nonsense mutation in the C-terminus of the PDE6β subunit, leading to truncation of the gene product and a nonfunctional PDE6 holoenzyme.[20,21] While previous studies in dogs have shown that PDE6β-RP is associated with rapid rod photoreceptor degeneration followed by progressive cone loss, the extent of retinal remodeling, the affected cell layers, the spatiotemporal distribution of photoreceptor degeneration, and the kinetics of these changes are still relatively unknown.[22,23] We recently demonstrated that subretinal injection of AAV2/5 or AAV2/8-RK.cpde6β in PDE6β-deficient dogs results in the concomitant long-term preservation of photoreceptor function and vision for at least 18 months.[23]

In the present study, we provide a detailed assessment of the long-term effects of subretinal gene therapy on the spatiotemporal pattern of cellular degeneration in treated PDE6β-deficient dogs. Moreover, we provide evidence of remarkable preservation of the retinal structure within the treated area over a 3.5-year period.

RESULTS

Gene therapy provides long-term visual function

In our previous study, 20-day-old rcd1 dogs were subretinally injected with rAAV vectors carrying the canine *Pde6β* gene under control of the photoreceptor-specific human rhodopsin kinase (RK) promoter.[23] In that study, we evaluated the retinal function and vision of treated dogs at specific time points up to 18 months postinjection. The present study followed four of those AAV2/5-treated dogs (T10-T13) to study the long-term effects of gene transfer on retinal structure (**Table 1**). Retinal function was evaluated using simultaneous bilateral full-field flash ERG up to 40 months postinjection (**Figure 1a**,**b**). Control recordings were obtained from healthy controls (PDE6β$^{+/-}$ dogs) and untreated contralateral eyes from PDE6β$^{-/-}$ dogs (**Table 1**). The mean scotopic b-wave amplitude in treated retinas was 52 ± 7 μV (n = 3) at 40 months postinjection (mpi) (**Figure 1c**), indicating prolongation of rod function. Moreover, these retinas showed b-wave amplitude that equated to 20–25% of the ERG amplitude measured in healthy eyes and persisted stably for at least 3 years after initial gene delivery (**Figure 1c**). Rod responses were undetectable in untreated contralateral eyes. All treated eyes showed a robust and stable preservation of cone function up to 40 months postinjection (**Figure 1d**). The mean amplitude of the 30 Hz flicker parameter for treated eyes at 40 mpi (32 ± 4 μV, n = 3) was 60–70% of the normal range of ERG values observed for healthy retinas (**Figure 1d**). By contrast, a progressive decrease in cone ERG amplitude was observed in all untreated contralateral eyes from approximately 9–40 months of age, at which point it was barely detectable (<10 μV and undetectable in one dog) (**Figure 1d**).

Table 1 Dogs used in the study: *in vivo* and postmortem analyses performed are indicated

Group	Animal	Age at euthanasia (months)	*In vivo* and postmortem analysis
Healthy dogs	H1	8	IHC, OCT
	H2	30	ERG, WM
	H3	15	WM
	H4	Still alive	ERG
	H5	Still alive	ERG
	H6	96	IHC
Untreated rcd1 dogs	U1	4	IHC
	U2	12	IHC
	U3	14	IHC
	U4	42	WM
	U5	78	IHC
	U6	96	IHC
Treated rcd1 dogs	T10, U10	42	ERG, OCT, WM
	T11, U11	42	ERG, OCT, IHC
	T12	32	ERG, OCT, WM
	T13, U13	39	ERG, OCT, IHC

ERG, electroretinogram; IHC, immunohistochemistry; OCT, optical coherence tomography; T, treated; U, untreated contralateral; WM, whole-mount imaging.

Natural history of degeneration in rcd1 dogs

First, we evaluated the natural history of degeneration by analyzing the 3 retinal nuclear layers in rcd1 dogs aged 4 months to 3.5 years (**Supplementary Figures S1 and S2**). Six matched retinal regions in the inferior, superior, and central retina (visual streak) were precisely analyzed (**Figure 2a**). Spatiotemporal patterns of degeneration were determined by quantifying rows of photoreceptor nuclei in the outer nuclear layer (ONL), rows of inner nuclear layer (INL) nuclei, and Neu-N-positive cells in the ganglion cell layer (GCL) (**Supplementary Figures S1 and S2**). In the peripheral retina, a rapid loss of nuclear rows in the ONL was observed at 4 months of age (4-month-old rcd1 dogs: 4 ± 1 rows; healthy controls (n = 2, 8, and 96 months of age): 10 ± 1; **Supplementary Figure S2**). By 12 months of age, the ONL had virtually disappeared in rcd1 dogs, with only 1–2 rows of nuclei remaining, and photoreceptors in the peripheral retina had lost both their outer and inner segments (**Supplementary Figure S1c**). The INL and GCL were similar to those of healthy retinas (**Supplementary Figures S1c and S2**). However, examination of retinal sections from 3.5-year-old rcd1 dogs revealed thin, gliotic retinas lacking retinal nuclear layers in the periphery and mild periphery (**Supplementary Figure S1e**).

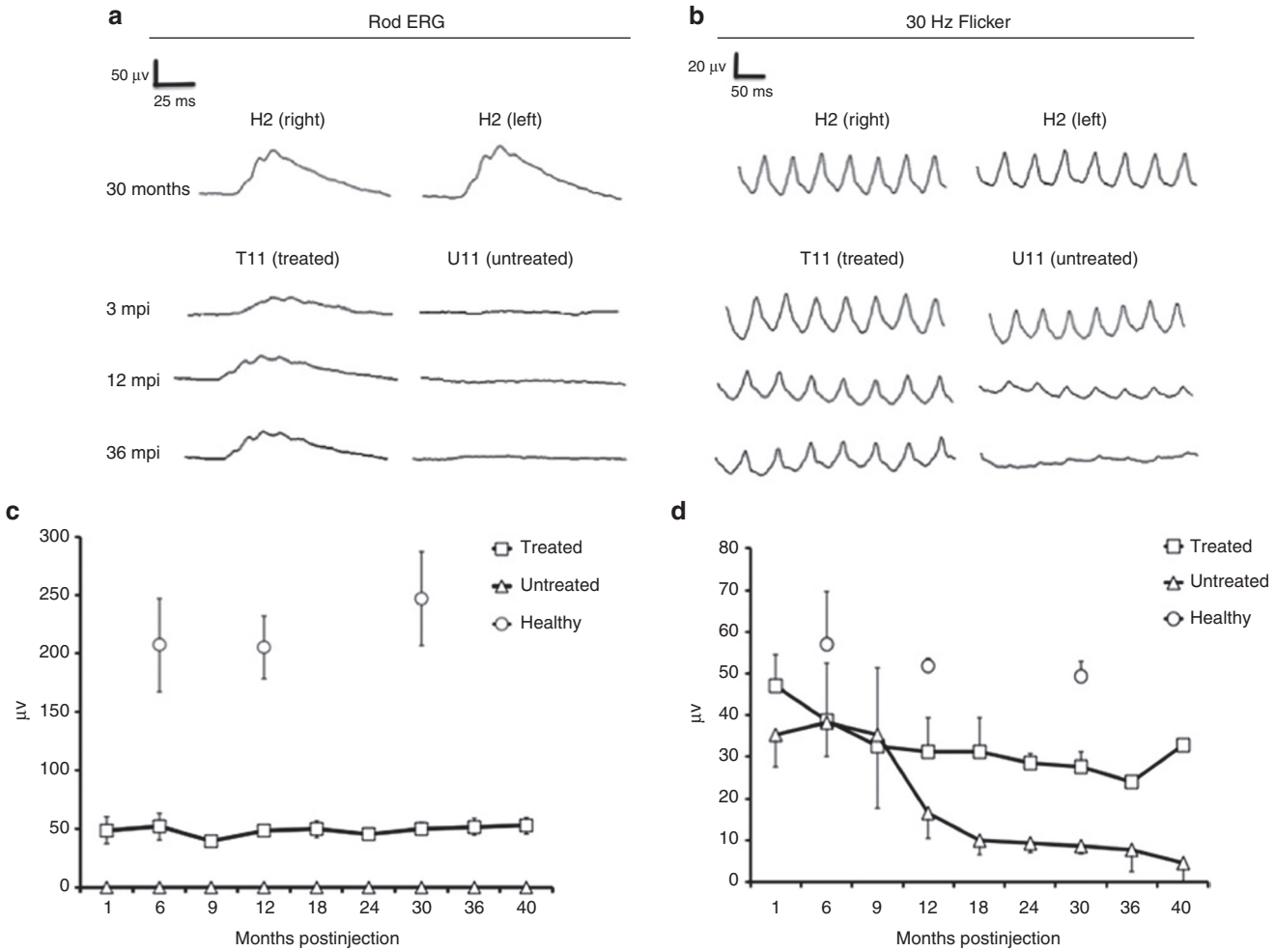

Figure 1 Kinetics of rod function restoration and cone function preservation in treated dogs. (**a,b**) Rod b-wave responses (**a**) and cone b-wave responses (**b**): electroretinographic traces from a healthy control (H2) at 30 months of age and from a rcd1 dog (treated and untreated eyes) at 3, 12, and 36 months postinjection. (**c,d**) Averaged rod-mediated (**c**) and cone-mediated (**d**) b-wave amplitudes from healthy retinas (n = 3) (○), treated retinas (□) (n = 3), and untreated retinas (△) (n = 3) over a 40-month period after injection. Symbols and bars represent mean ± SD. ERG, electroretinogram; mpi, month(s) postinjection.

By this stage, only the visual streak contained a few rows of photoreceptor nuclei that persisted in the ONL (3.5-year-old rcd1 dogs: 1.5 ± 0.5 rows; healthy controls: 12 ± 2 rows), with total preservation of the INL and ganglion cells (**Supplementary Figure S1f**). Indeed, the INL (4 ± 1 rows) and NeuN-positive retinal ganglion cells (RGCs) (47 ± 11 per mm) were similar to those of healthy controls (rows in INL: 5 ± 1; NeuN-positive RGCs: 36 ± 3 per mm; **Supplementary Figure S2**).

Effect of gene therapy on retinal nuclear layer organization

To evaluate the effect of gene transfer on retinal structures, ONL and INL nuclei and NeuN-positive RGCs were counted in six retinal regions (**Figure 2a**). Entire retinas of treated rcd1 dogs collected more than 3 years after vector injection were compared with untreated contralateral retinas, and retinas of healthy dogs (n = 2, 8, and 96 months of age) (**Table 1**). Histological analyses revealed dramatic differences in the retinal morphology between treated and untreated retinas (**Figure 2b**). In transduced peripheral retinas, we observed preservation of the retinal structures, including the 3 nuclear layers, whereas untreated peripheral retinas had completely degenerated (**Figure 2b**, **Supplementary Figure S3**). Interestingly, quantitative analysis revealed that the average number of rows of photoreceptor nuclei in the peripheral retina of 3.5-year-old treated rcd1 dogs was similar to that in the same region of 4-month-old rcd1 dogs (3.5 years old: 6 ± 0.8 rows; 4 months old: 6 ± 1 rows; **Figure 3a**). Furthermore, count values indicated total preservation of the number of cell rows in the INL (3 ± 0.8) and the number of NeuN-positive RGCs (7 ± 2) in treated peripheral retinas (healthy control retinas: rows in INL, 3 ± 2; NeuN-positive RGCs, 6 ± 2; **Figure 3b**,**c**). In the transduced visual streak, the ONL contained 5 ± 0.8 rows of nuclei (three times that of the untreated visual streak: 1.5 ± 0.5 rows), which equated to ~50% of the ONL thickness in the visual streak of healthy retinas (12 ± 2 rows) (**Figures 2b** and **3a**).

Rod and cone preservation in response to gene therapy

To evaluate the long-term effect of gene therapy on photoreceptor preservation, we analyzed rod and cone segments in

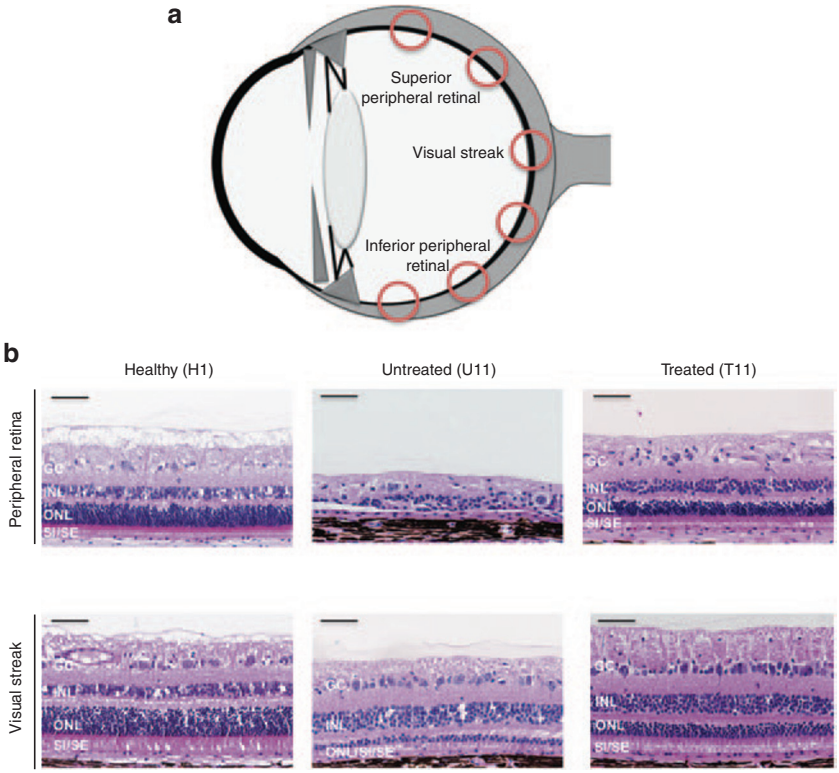

Figure 2 Effect of gene therapy on retinal nuclear layer organization. (**a**) Schematic section of the entire retina. Red circles represent the different areas examined. (**b**) Retinal cross-sections (in peripheral or visual streak) from a healthy dog (H1, 8 months of age) and a 3.5-year-old rcd1 dog (treated and untreated eyes) indicating the extent of degeneration in the three retinal layers. All magnifications: 40× objective, zoom 1.0 (scale bars, 100 µm). GC, ganglion cells; INL, inner nuclear layer; ONL, outer nuclear layer; IS/OS, inner and outer segments.

whole-mount retinas using specific markers for rods and cones (GNAT1 and Peanut lectin agglutinin (PNA), respectively) in 3.5-year-old rcd1 dogs (treated retina and untreated contralateral retina) and in healthy retinas (n = 2, 15, and 30 months of age) (**Table 1**, **Figure 4**). Focal plane images were acquired at the rod and cone segment level (**Figure 4**). Fluorescence microscopy of whole-mount retinas revealed preservation of rods and cones in vector-exposed rcd1 retinas. Photoreceptor preservation was limited to treated areas (**Figure 4c**,**j**,**k**). The size of the retinal bleb was approximately 25–35% of the entire retina, in agreement with OCT analysis of treated rcd1 dog retinas (n = 4) (data not shown). Rods were completely absent outside the treated region and in untreated contralateral retinas (**Figure 4b**). Similarly, cones were absent outside the bleb (**Figure 4i**) and in the peripheral retina of untreated eyes (**Figure 4h**). Interestingly, residual cones were observed in the visual streak of untreated retinas (**Figure 4g**), in line with previous histological findings, providing new evidence of a preserved area in untreated rcd1 dogs of 3 years and older. However, confocal analysis revealed that these cones had lost their original shape and contained shorter segments than the cones of the area centralis (**Figure 4e**) and visual streak (**Figure 4f**) of healthy retinas or treated rcd1 retinas (**Figure 4j**). To precisely characterize photoreceptor preservation, we further analyzed the morphology and density of rod and cone subtypes throughout the entire retina by immunohistochemistry. Rod segments and L/M- or S-cone opsin-positive outer segments were analyzed using rod-specific markers (GNAT1) and M- and S-cone opsin-specific antibodies (**Figure 5**). No GNAT1 labeling was observed in untreated retinas in either the peripheral retina or visual streak (**Figure 5b**,**k**), confirming the complete absence of rods in rcd1 dogs of more than 3 years of age.

Interestingly, while the peripheral region was completely degenerated in untreated retinas (**Figure 5b**,**e**,**h**), we observed preservation of L/M- and S-cone segments in the visual streak of untreated retinas (**Figure 5n**,**q**). No mislocalization of cone opsins was observed in the inner segment or cell bodies. However, structural analysis revealed morphological differences between outer and inner photoreceptor segments: outer and inner segments were shortened and morphologically anomalous, and outer segments were bulbous in shape (**Figure 5n**,**q**). Quantitative analysis revealed fewer L/M- and S-opsin-positive cone outer segments in the visual streak of untreated retinas versus healthy retinas (**Figure 6a**,**b**). This difference was more pronounced for S cones: only 35% of S cones were maintained in the visual streak of untreated retinas (untreated: 7 ± 3 S cones per mm; healthy: 19 ± 3 S cones per mm; **Figure 6b**).

While immunohistochemistry revealed a total absence of rods in 3.5-year-old untreated rcd1 dogs (**Figure 5b**,**k**), significant preservation of rods was observed in the peripheral and central areas of vector-exposed retinas (**Figure 5c**,**l**). Quantification of rod segments was hampered by their high density and small size. However, rod density in vector-exposed retinas (**Figure 5c**,**l**) was markedly lower than in healthy retinas (**Figure 5a**,**j**). These observations were consistent with our histological findings demonstrating a

loss of nuclear rows in the ONL (Figure 2b). Moreover, in vector-exposed retinas, immunohistochemistry revealed the presence of normal cone structures with no mislocalization of cone opsins in the inner segments or cell bodies (Figure 5f,i,o,r). L/M- and S-cones were preserved in treated peripheral retinas (Figure 5f,i). By contrast, all cone photoreceptor subtypes were completely lost in untreated peripheral retinas (Figure 5e,h). Quantitative analysis revealed more L/M- and S-opsin-positive cone outer segments in the visual streak of vector-exposed versus untreated retinas (treated: 172 ± 22 L/M and 24 ± 3 S cones per mm; untreated: 129 ± 26 L/M and 7 ± 3 S cones per mm; Figure 6a,b). Lastly, the outer segment of the 2 cone subtypes in vector-exposed retinas (peripheral retina or visual streak) were completely preserved (Figure 6a,b); cone density in treated peripheral retinas was comparable to that seen in the same region in healthy retinas (treated: 9 ± 5 S cones and 101 ± 23 L/M cones per mm; healthy: 7 ± 4 S cones and 88 ± 7 L/M cones per mm; Figure 6a,b). Similarly, both cone subtypes were completely preserved in the visual streak of treated retinas (treated: 24 ± 3 S cones and 172 ± 23 L/M cones per mm; healthy: 19 ± 7 S cones and 178 ± 6 L/M cones per mm). Finally, although cone morphology and number were maintained in vector-exposed retinas, we noted a slight decrease in the number of cones at the border of the treated region as compared with the same region in healthy retinas (treated retinas: 4 ± 1 S cones and 58 ± 8 L/M cones per mm; healthy retina: 9 ± 4 S cones and 80 ± 15 L/M cones per mm; Figure 6a,b).

Effect of gene therapy on inner layers and retinal glia

To examine the effect of gene transfer on the inner retinal neurons, bipolar and horizontal cells were labeled using antibodies against PKCα and calbindin, respectively. We also used glial markers (anti-GS and anti-glial fibrillary acidic protein antibodies) to examine Müller cell structure and reactivity, respectively. The morphology and immunocytochemistry of the peripheral retina of 3.5-year-old rcd1 dogs (untreated and vector-exposed) and healthy controls (n = 2, 15, and 30 months of age) was assessed (Figure 7). In vector-exposed retinas, PKCα staining was observed in the dendrites projecting toward the rod terminals, and calbindin immunoreactivity was detected in the OPL, horizontal cell bodies, and their dendrites (Figure 7c,f). By contrast, no PKCα or calbindin labeling was observed in any part of the untreated peripheral retina (Figure 7b,e). Interestingly, similar patterns of PKCα and calbindin staining were observed in healthy and vector-exposed retinas (Figure 7a,d,c,f). Müller cell labeling was only detectable in vector-exposed retinas (Figure 7h,i), whereas glial fibrillary acidic protein was expressed by retinal astrocytes in both untreated and vector-exposed retinas (Figure 7l,k). We observed no appreciable variation in the expression and distribution of Müller cell markers in vector-exposed retinas as compared with healthy controls: GS antibodies labeled all Müller glial cells, including the soma, processes, and end feet in the inner and outer limiting membranes (Figure 7i). Immunohistochemistry thus revealed a striking preservation of retinal glia and inner layers after AAV-mediated gene therapy.

DISCUSSION

In a previous study, we reported that rAAV 2/5-mediated cPDE6β expression in a large animal model of severe rod-cone dystrophy, the rcd1 dog, resulted in concomitant preservation of photoreceptor function and vision for at least 18 months.[23] In the present study, we investigated in detail the effect of gene transfer on retinal structures 3.5 years after treatment. We show that gene replacement therapy in PDE6β-deficient dogs successfully protects the retina against progressive degeneration.

Despite several successful gene therapy interventions in murine models of PDE6β-deficiency,[17,18] these models have some limitations for study of the specific long-term effects of gene

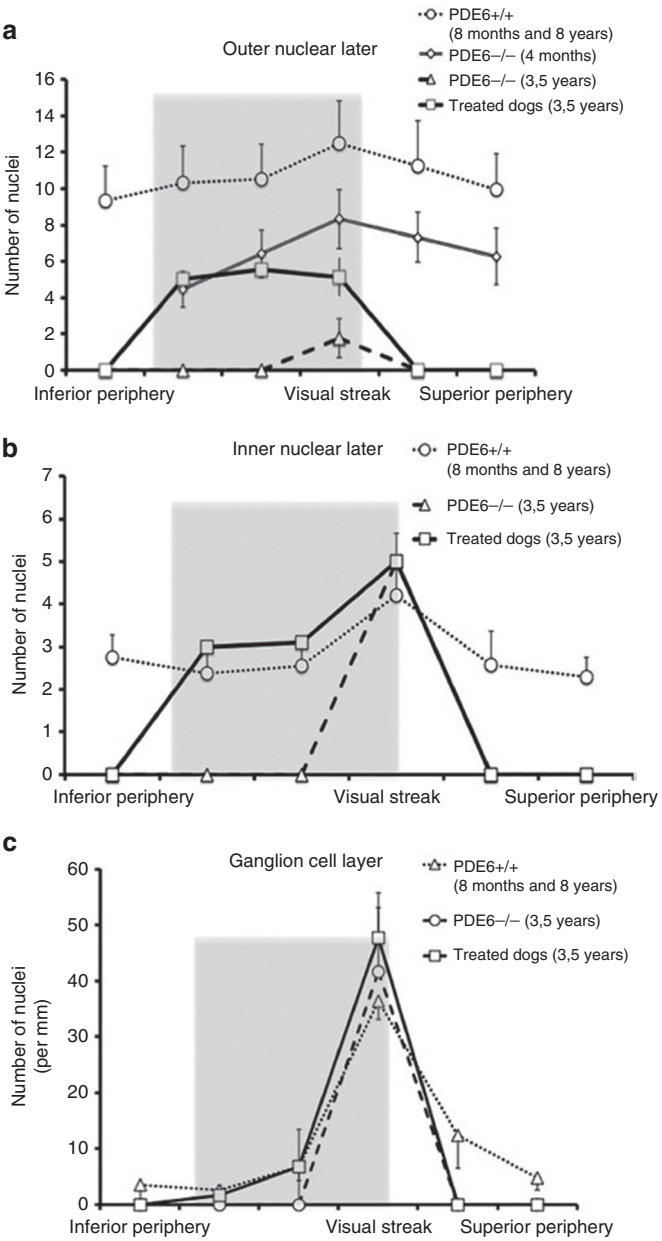

Figure 3 Density of retinal nuclear layers in treated rcd1 dogs. Quantification of ONL nuclei (**a**), INL cells (**b**), and NeuN-positive RGCs (**c**) were performed in six retinal regions from 3.5-year-old rcd1 dogs (treated eyes (□) and untreated contralateral eyes (△)). Treated eyes were compared with retinas from healthy dogs (n = 2, 8 months and 8 years of age) (○) and unaffected 4-month-old rcd1 dogs (◊). Values represent the mean ± SD. The shaded portion represents the location of the vector-exposed area. RGC, retinal ganglion cell.

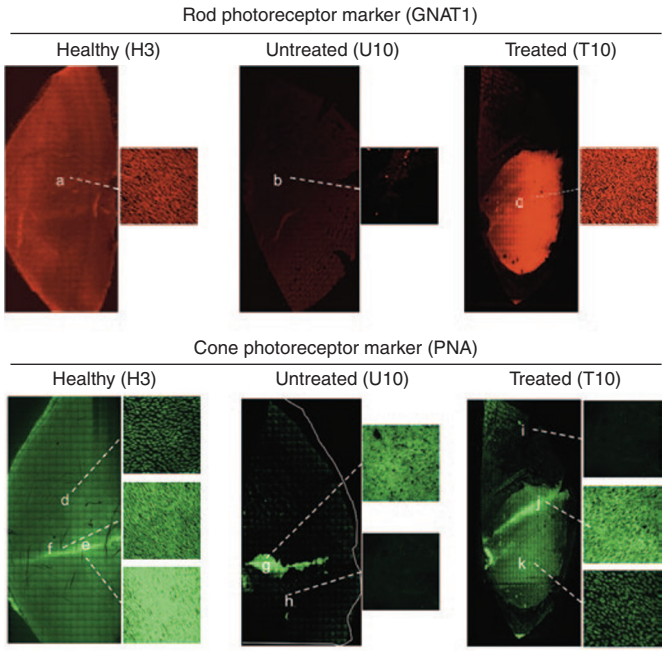

Figure 4 Spatial distribution of rods and cones as observed in retinal whole mounts. Rod and cone distribution was analyzed in healthy dog (H3, 15 months of age) and 3.5-year-old-treated rcd1 dog (U10, T10). Retinal flat mounts were stained with GNAT1 and peanut agglutinin (PNA) antibody, which specifically label rods (red) and cones (green), respectively. (**a–c**) Rod density in healthy retina and rcd1 retinas (treated and untreated contralateral). (**d,h,i**) Cone density in peripheral retinas: healthy, rcd1 (treated and untreated contralateral retinas). (**e,f**) Cone density in the visual streak and area centralis, the site of maximum photoreceptor density, in healthy retina. (**g**) Preserved area in untreated rcd1 retina. (**j**) Cone density in the visual streak of treated rcd1 retina. (**k**) Cone density in treated areas.

therapy in PDE6β-RP. Nocturnal species, including PDE6β-deficient mice, possess very few cones, and most coexpress both S and M opsins in the retina, in contrast to dogs or humans.[24,25] Moreover, unlike human and dog retinas, the mouse retina lacks a cone-rich region.[19,26] SD-OCT evaluation of morphological alterations in PDE6β-RP patients has revealed massive rod loss.[10,27] Studies of the retinas of RP donor patients with different forms of RP have shown that monolayers of cone somata are still detectable in the fovea in advanced stages of the disease.[28–30] These cones have very short outer segments and exhibit aberrant morphologies, with bulbous outer segments. To our knowledge, no study has precisely evaluated the kinetic patterns of retinal degeneration in the rcd1 dog model. Here, we describe the extent of retinal remodeling, the affected cell layers, and the spatiotemporal distribution of photoreceptor degeneration in the rcd1 dog. Interestingly, as described in PDE6β-RP patients, the visual streak of 3.5-year-old rcd1 dogs retained a monolayer of cone somata consisting of shortened segments, whereas the retina was completely degenerated in both the periphery and mid periphery. Our study further characterized the preserved area by demonstrating the presence of L/M- and S-opsin-positive cone outer segments in the visual streak of rcd1 dog retinas up to 6 years of age (data not shown). The synthesis of opsin and the preservation of INL and GCL in the visual streak may explain why rcd1 dogs show no signs of visual impairment in bright light up to at least 6 years of age (data not shown), despite cone function undetectable by ERG. Our findings suggest that the long-term preservation of cones in the rcd1 dog mimics the spatiotemporal distribution of photoreceptor degeneration, in particular the preservation of foveal cones observed in patients in advanced stages of retinal degeneration.[28–30] Given the scarcity of human postmortem retina samples, this model could help elucidate the mechanisms that underlie cone loss in this RP subset caused by a rod-specific mutation, and mediate the survival of a few functional cones in the central retina. Little is known about the molecules that mediate cone cell death or promote cone protection in the latter stages of rod cone dystrophies, particularly in the vast majority of cases in which the causal mutation only affects rods.[31–34]

We have evaluated the effect of gene transfer at over 3 years post-treatment in rcd1 dogs. The effects of gene therapy on photoreceptor survival have been recently studied in RPE65-deficient dogs. However, that model, in contrast to the rcd1 dog, is characterized by slow photoreceptor degeneration,[35,36] which is detectable by OCT at 5 years of age.[35] The advantage of the rcd1 model is that the effect of gene transfer on retinal structures can be observed within a short time frame owing to the severity of the degeneration. In this model, we identified the retinal bleb, which represents approximately 25–35% of the entire retina. Surprisingly, while no rods were observed outside the bleb or in the untreated contralateral eye, gene transfer halted rod degeneration in all vector-exposed regions for at least 3.5 years post-treatment. This preservative effect was not complete, as approximately 50% of the rod nuclei in the ONL were lost. The fact that rod death is not entirely prevented is unsurprising, as rod degeneration is already underway before maximum transgene expression is achieved (over 50% of rods are already lost by 4 months of age in untreated rcd1 dogs). Strikingly, PDE6β gene therapy resulted in total preservation of L/M and S cones. By contrast, no photoreceptors remained in vector-unexposed retinas, except for 1–2 rows of cones in the visual streak. Moreover, while loss of the INL and GCL, were observed outside the retinal bleb, no degeneration of these retinal layers was observed in vector-exposed regions. Finally, we found that the retinal structure of 3.5-year-old treated rcd1 dogs was almost completely preserved, and was almost identical to that of 4-month-old rcd1 dogs. While photoreceptor degeneration is prevented in RPE65-deficient dogs treated with gene therapy between 1 and 28 months of age (*i.e.*, before the onset of retinal degeneration),[36–39] treatment administration at 4.8 years of age or older (*i.e.*, during the retinal degeneration stage) fails to prevent continuous photoreceptor loss in the long term.[35] In line with previous findings in RPE65-deficient dogs treated during the retinal degeneration stage, recent studies have demonstrated temporary improvements in retinal sensitivity after gene therapy using rAAV2/2.hRPE65 in patients with retinal dystrophy caused by mutations in the *RPE65* gene. However, between 6 months and 3 years after treatment, retinal sensitivity declines and photoreceptor loss is observed in all patients.[35,40,41] The reasons underlying this decline are unknown. Moreover, no clear correlation between gene therapy response and patient age has been observed. One hypothesis is that the amount of RPE65 protein may be insufficient to promote a long-term effect. Alternatively, this effect may be due to suboptimal timing of the intervention. Indeed, in clinical trials patients received

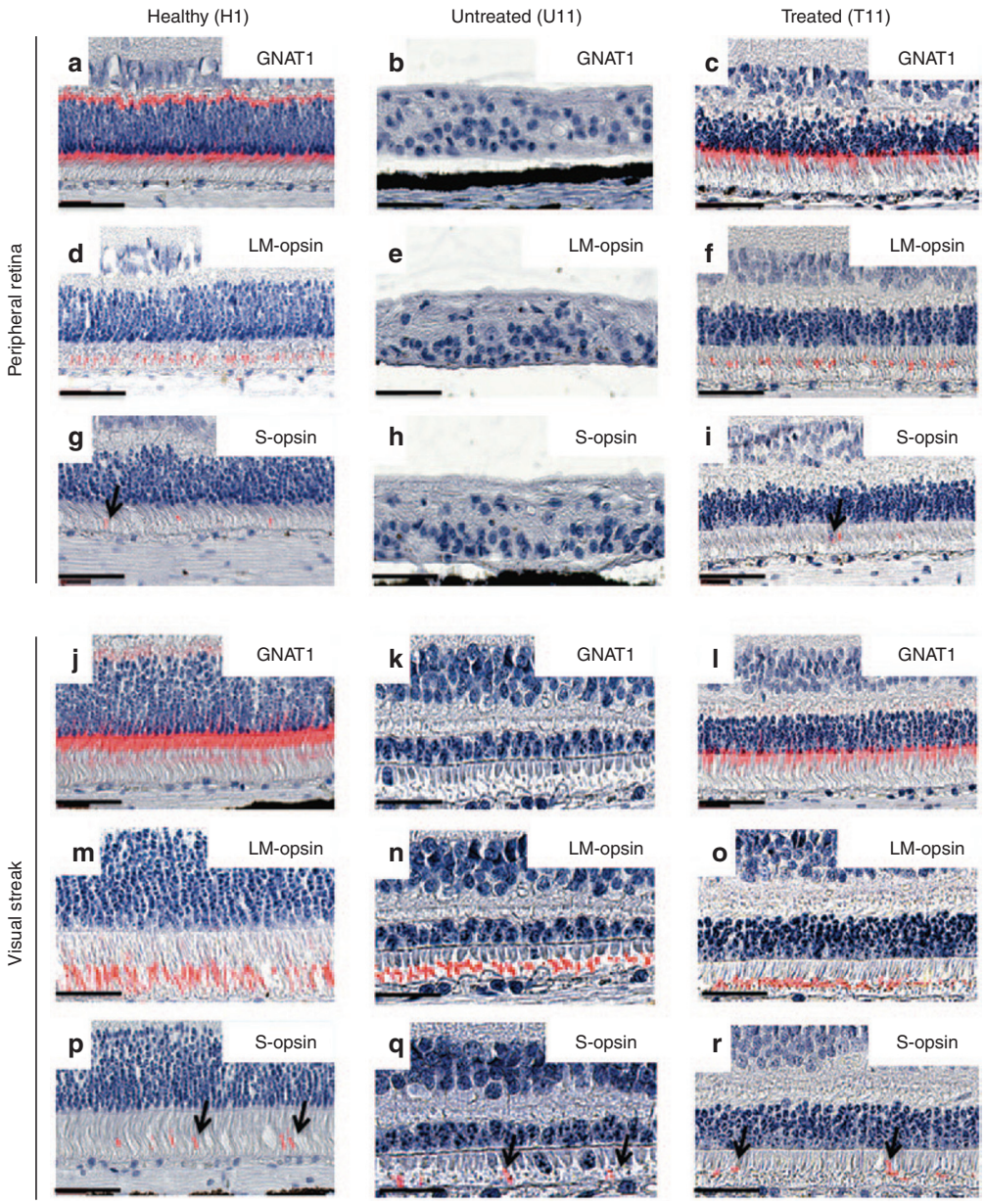

Figure 5 Morphology and density distribution of rod and cone subtypes in retinal sections. Paraffin-embedded retina sections from healthy dogs (*n* = 2, 8 months and 8 years of age) and a 3.5-year-old rcd1 dogs (treated and untreated contralateral retina) were stained using rod-specific markers (GNAT1) or L/M- and S-opsin-specific antibodies. Histochemical detection of rod segments in healthy (H1, 8 months of age) and treated rcd1 (T11) retinas: peripheral retinas (**a,c**), and the visual streak (**j,l**). Absence of rods in untreated rcd1 retina (U11) (**b,k**). L/M- and S-opsin staining in peripheral retinas (**d,f,g,i**) and the visual streak (**n,o,p,r**) in healthy eyes and treated rcd1 eyes. No detectable L/M or S-opsin expression was detected in the peripheral retina of untreated rcd1 eyes (**e,h**). Immunohistochemistry detection of cone segments in the preserved area of untreated rcd1 retinas (**n,q**). Black arrows indicate S-opsin-positive cone outer segments. Magnifications: 40× objective, zoom 2.0 (scale bars, 50 µm). Sections were counterstained with Mayer's hemalum. Merged image shows a combination of fluorescence and Mayer's hemalum staining.

gene therapy during neuronal degeneration. Thus, AAV-mediated RPE65 gene therapy may fail to arrest the degenerative process if the intervention occurs after the onset of photoreceptor degeneration. Our results for AAV-mediated PDE6β gene therapy indicate that although degeneration is already underway by the time transgene expression peaks, further retinal degeneration is prevented by gene transfer. These findings are in good agreement with those of Koch and coworkers, who recently generated an inducible transgenic mouse PDE6β-RP model in which the *PDE6β* gene can be uniformly delivered to all rod photoreceptors after tamoxifen administration. They demonstrated sustained rescue of photoreceptor structures, even when tamoxifen was administered in mild or even late-stage disease stages.[42] These observations support our findings in a natural dog model of PDE6β-RP, and indicate that vector administration prior to total rod loss may provide long-term beneficial effects for PDE6β-RP patients.

In conclusion, our analyses demonstrate that severe, long-term retinal degeneration can be unequivocally prevented by gene therapy in PDE6β-deficient dogs over a 3.5-year period. That these results were obtained in a highly degenerative model is

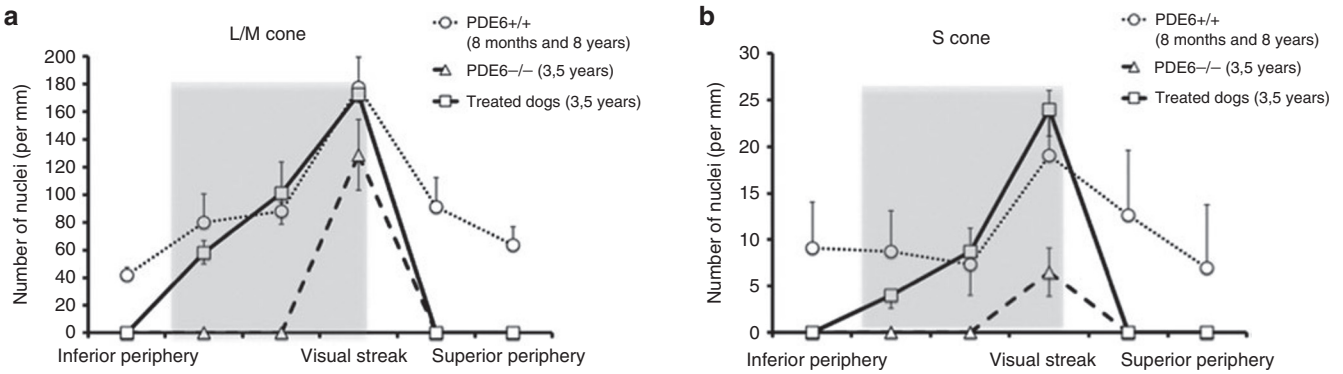

Figure 6 Density of cone subtypes in treated rcd1 retinas. L/M-cone subtypes (**a**) and S-cone subtypes (**b**) were quantified in six retinal regions from 3.5-year-old rcd1 dogs (treated (□) and untreated contralateral (△) eyes). Treated eyes were compared with those of healthy controls (n = 2, 8 months and 8 years of age) (○). Data represent the mean ± SD. Shading indicates the location of vector-exposed areas.

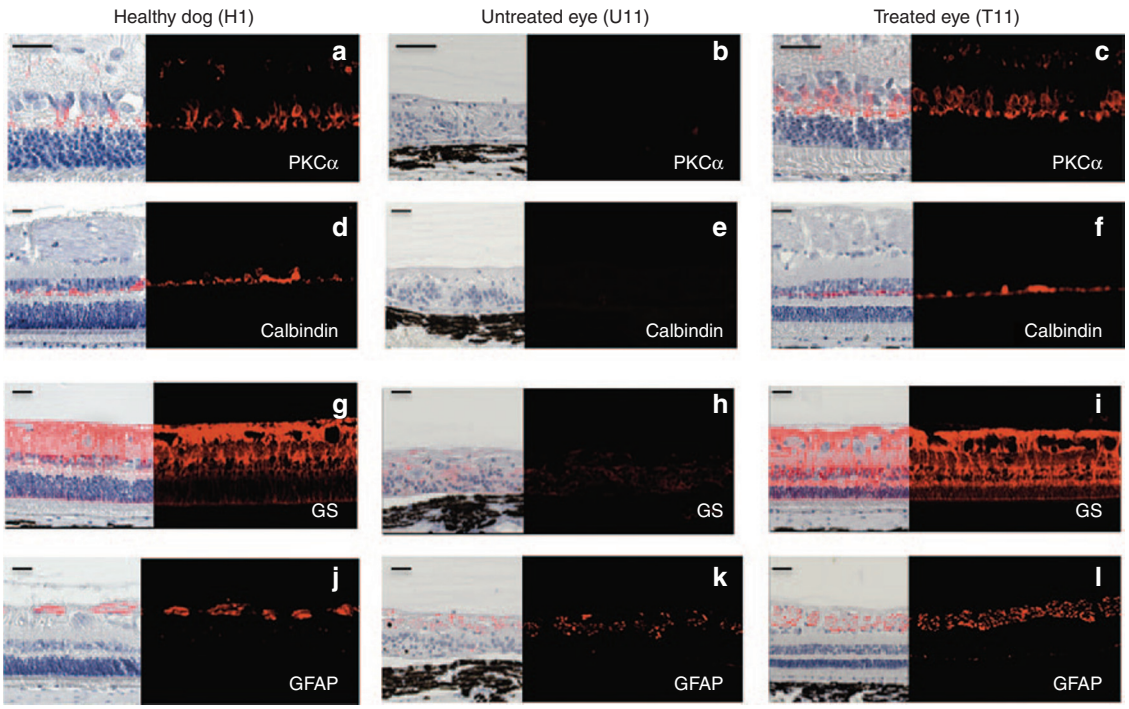

Figure 7 Effect of gene therapy on inner layer and retinal glia. Image showing immunohistochemistry in the peripheral retina of healthy controls (n = 2, 8 months and 8 years of age) and rcd1 dogs (untreated and vector-exposed retinas). Bipolar cells and horizontal cells were labeled using antibodies against PKC-α and calbindin, respectively (**a–f**). Glial cells were stained using anti-GS and anti-GFAP antibodies (**g–i**). Magnifications: 40× objective, zoom 1.0, except for PKC-α staining (40× objective, zoom 2.0) (scale bars, 50 µm). GFAP, glial fibrillary acidic protein.

encouraging, and points to significant potential for this therapeutic approach in future clinical trials.

MATERIALS AND METHODS

All experiments were performed under the control of our quality management system, which has been approved by Lloyd's Register Quality Assurance to meet the requirements of the international management system standard ISO 9001:2008. This covers a range of laboratory activities, including research experiments and the production of research-grade viral vectors.

Animals. Ten Pde6β$^{-/-}$ and six healthy dogs were used in this study (Table 1). The dog colony was kindly provided by D.J. Maskell (University of Cambridge, Cambridge, UK). Research was conducted at the Boisbonne Centre (ONIRIS, Nantes-Atlantic College of Veterinary Medicine, Nantes) under authorization #H44273 delivered by the Departmental Direction of Veterinary Services (Loire-Atlantique, France). All animals were handled in accordance with the Guide for the Care and Use of Laboratory Animals. The experiments involving animals were conducted in accordance with agreement #00724.01 delivered by the Animal Experimentation Ethics Committee of Pays de Loire (France) and the Ministry of Higher Education and Research.

ERG. Retinal function of treated Pde6β$^{-/-}$ dogs (treated eyes and untreated contralateral eyes) and healthy Pde6β$^{+/-}$ controls was evaluated using bilateral full-field flash ERG. Pupils were fully dilated by topical administration of tropicamide (Laboratoire Théa, France) and phenylephrine hypochloride (Laboratoire Théa, France). The dogs were dark-adapted for 20 minutes and anesthetized after premedication by intravenous injection of sodium thiopental (Specia Laboratories, Paris, France) followed by isofluorane gas inhalation. Hydroxypropulmethylcellulose (Laboratoires Theala, Clermont-Ferrand, France) was applied to each eye to prevent corneal

dehydration during recording, which was performed using a MonColor computer-based system (Metrovision, Pealrenchies, France) and contact lens electrodes (ERG-jet; Microcomponents SA, Grenchen, Switzerland). ERGs were recorded in a standardized fashion in accordance with the recommendations of the International Society for Clinical Electrophysiology of Vision,[43] using a protocol described previously.[44]

Whole-mount immunofluorescence. Dogs were euthanized by intravenous injection of sodium pentobarbital (Vealtoquinol, Lure, France), always at the same time of day and under fixed light conditions. Eyes were enucleated and both the anterior part and the lens were removed and fixed for 30 minutes in 4% paraformaldehyde in phosphate-buffered saline (PBS) solution. After washing, the neuroretina was removed from the RPE-choroid-sclera using a fine forceps. Retinas were then washed three times in PBS at room temperature and incubated in a mixture of PNA-FITC lectin antibody (1/250; Vector Laboratories, Peterborough, UK) and GNAT1 antibody (1/250; Santa Cruz Tebu Bio). After several washes in PBS, retinas were incubated for 2 hours at room temperature with 546-conjugated anti-rabbit IgG antibody (1/250; Life Technologies, Saint Aubin, France). Retinas were subsequently washed in PBS, mounted in Prolong Gold anti-fade reagent (Life Technologies) and stored at 4 °C until further microscopic analysis. Flat-mounted neuroretinas were examined using a laser scanning confocal microscope (Nikon A1RSi). Three-dimensional digital images were collected at 20× (NA 0.75) and 60× (NA 1.4) using NIS-Elements confocal software and appropriate fluorescence filters for excitation laser 488 and 561 nm. Twenty sections per retina, representative of the whole eye (from temporal to nasal side), were analyzed. In each slide, cell counts were performed in three areas each from six different regions (n = 360 areas counted per eye). All analyses were performed in duplicate, with each count performed by a different person.

Histological analysis and immunohistochemistry. Dogs were euthanized by intravenous injection of sodium pentobarbital (Vealtoquinol, Lure, France). Eyes were immediately enucleated, fixed for 48 hours in Bouin's solution, and embedded in paraffin. Entire retinas were cut into 5-µm sections. Morphological analysis was performed after hematoxylin and eosin staining. Various antibodies (listed in **Supplementary Table S1**) were used to identify the molecular markers that define the different layers of the retina (rod and cone photoreceptors, INL, GCL, and retinal glia). Sections were deparaffinized and rehydrated. Antigen was demasked by boiling the section in ready-to-use citrate-based epitope retrieval solution, pH 6.0 (AR9961, Leica Microsystems, Nanterre, France). Nonspecific activity was blocked by incubating the sections for 60 minutes at room temperature in 20% goat serum in PBS containing 0.1% Triton X-100. Sections were incubated overnight at 4 °C in primary antibody diluted in PBS (**Table 1**), washed three times for 5 minutes in PBS containing 0.1% Triton X-100, and incubated for 2 hours at room temperature in 546-conjugated anti-rabbit or anti-mouse IgG antibody (Life Technologies). After washing, the nuclei were counterstained with Mayer's hemalum solution and the slides were mounted in Prolong Gold anti-fade reagent (Life Technologies). Stained slides were scanned using the Hamamatsu NanoZoomer (Bacus Laboratories, Chicago, IL) and analyzed using NDP.View2 software. Mayer's hemalum staining and the corresponding fluorescence image were merged using Fiji software (http://fiji.sc).

SUPPLEMENTARY MATERIAL

Figure S1. Natural history of degeneration in rcd1 dogs.
Figure S2. Temporal course of degeneration in rcd1 dogs.
Figure S3. Histochemical detection of NeuN-positive RGCs in a healthy dog (H1) and in a 3.5-year-old rcd1 dog (treated and untreated contralateral retinas).
Table S1. List of the antibodies used in the study.

ACKNOWLEDGMENTS

We thank K. Stieger (Justus-Liebig University, Giessen, Germany) for his critical reading of this manuscript and Mireille Ledevin for the retinal sections. We also thank the staff of the Boisbonne Center for animal care, the MicroPICell platform (Nantes University, IFR26) for technical assistance and assistance with confocal microscopy and retinal sections. This work was supported by the Association Française contre les Myopathies, INSERM, and the Fondation d'Entreprises pour la Thérapie Génique en Pays de la Loire. The authors declare no conflict of interest

REFERENCES

1. Sancho-Pelluz, J, Arango-Gonzalez, B, Kustermann, S, Romero, FJ, van Veen, T, Zrenner, E *et al.* (2008). Photoreceptor cell death mechanisms in inherited retinal degeneration. *Mol Neurobiol* **38**: 253–269.
2. Danciger, M, Heilbron, V, Gao, YQ, Zhao, DY, Jacobson, SG and Farber, DB (1996). A homozygous PDE6B mutation in a family with autosomal recessive retinitis pigmentosa. *Mol Vis* **2**: 10.
3. McLaughlin, ME, Sandberg, MA, Berson, EL and Dryja, TP (1993). Recessive mutations in the gene encoding the beta-subunit of rod phosphodiesterase in patients with retinitis pigmentosa. *Nat Genet* **4**: 130–134.
4. McLaughlin, ME, Ehrhart, TL, Berson, EL and Dryja, TP (1995). Mutation spectrum of the gene encoding the beta subunit of rod phosphodiesterase among patients with autosomal recessive retinitis pigmentosa. *Proc Natl Acad Sci USA* **92**: 3249–3253.
5. Hartong, DT, Berson, EL and Dryja, TP (2006). Retinitis pigmentosa. *Lancet* **368**: 1795–1809.
6. Clark, GR, Crowe, P, Muszynska, D, O'Prey, D, O'Neill, J, Alexander, S *et al.* (2010). Development of a diagnostic genetic test for simplex and autosomal recessive retinitis pigmentosa. *Ophthalmology* **117**: 2169–77.e3.
7. Danciger, M, Blaney, J, Gao, YQ, Zhao, DY, Heckenlively, JR, Jacobson, SG *et al.* (1995). Mutations in the PDE6B gene in autosomal recessive retinitis pigmentosa. *Genomics* **30**: 1–7.
8. Collin, RW, van den Born, LI, Klevering, BJ, de Castro-Miró, M, Littink, KW, Arimadyo, K *et al.* (2011). High-resolution homozygosity mapping is a powerful tool to detect novel mutations causative of autosomal recessive RP in the Dutch population. *Invest Ophthalmol Vis Sci* **52**: 2227–2239.
9. Tsang, SH, Tsui, I, Chou, CL, Zernant, J, Haamer, E, Iranmanesh, R *et al.* (2008). A novel mutation and phenotypes in phosphodiesterase 6 deficiency. *Am J Ophthalmol* **146**: 780–788.
10. Jacobson, SG, Sumaroka, A, Aleman, TS, Cideciyan, AV, Danciger, M and Farber, DB (2007). Evidence for retinal remodelling in retinitis pigmentosa caused by PDE6B mutation. *Br J Ophthalmol* **91**: 699–701.
11. Bennett, J, Tanabe, T, Sun, D, Zeng, Y, Kjeldbye, H, Gouras, P *et al.* (1996). Photoreceptor cell rescue in retinal degeneration (rd) mice by *in vivo* gene therapy. *Nat Med* **2**: 649–654.
12. Jomary, C, Vincent, KA, Grist, J, Neal, MJ and Jones, SE (1997). Rescue of photoreceptor function by AAV-mediated gene transfer in a mouse model of inherited retinal degeneration. *Gene Ther* **4**: 683–690.
13. Kumar-Singh, R and Farber, DB (1998). Encapsidated adenovirus mini-chromosome-mediated delivery of genes to the retina: application to the rescue of photoreceptor degeneration. *Hum Mol Genet* **7**: 1893–1900.
14. Takahashi, M, Miyoshi, H, Verma, IM and Gage, FH (1999). Rescue from photoreceptor degeneration in the rd mouse by human immunodeficiency virus vector-mediated gene transfer. *J Virol* **73**: 7812–7816.
15. Pang, JJ, Boye, SL, Kumar, A, Dinculescu, A, Deng, W, Li, J *et al.* (2008). AAV-mediated gene therapy for retinal degeneration in the rd10 mouse containing a recessive PDEbeta mutation. *Invest Ophthalmol Vis Sci* **49**: 4278–4283.
16. Allocca, M, Manfredi, A, Iodice, C, Di Vicino, U and Auricchio, A (2011). AAV-mediated gene replacement, either alone or in combination with physical and pharmacological agents, results in partial and transient protection from photoreceptor degeneration associated with betaPDE deficiency. *Invest Ophthalmol Vis Sci* **52**: 5713–5719.
17. Pang, JJ, Dai, X, Boye, SE, Barone, I, Boye, SL, Mao, S *et al.* (2011). Long-term retinal function and structure rescue using capsid mutant AAV8 vector in the rd10 mouse, a model of recessive retinitis pigmentosa. *Mol Ther* **19**: 234–242.
18. Nishiguchi, KM, Carvalho, LS, Rizzi, M, Powell, K, Holthaus, SM, Azam, SA *et al.* (2015). Gene therapy restores vision in rd1 mice after removal of a confounding mutation in Gpr179. *Nat Commun* **6**: 6006.
19. Mowat, FM, Petersen-Jones, SM, Williamson, H, Williams, DL, Luthert, PJ, Ali, RR *et al.* (2008). Topographical characterization of cone photoreceptors and the area centralis of the canine retina. *Mol Vis* **14**: 2518–2527.
20. Suber, ML, Pittler, SJ, Qin, N, Wright, GC, Holcombe, V, Lee, RH *et al.* (1993). Irish setter dogs affected with rod/cone dysplasia contain a nonsense mutation in the rod cGMP phosphodiesterase beta-subunit gene. *Proc Natl Acad Sci USA* **90**: 3968–3972.
21. Aguirre, G (1978). Retinal degenerations in the dog. I. Rod dysplasia. *Exp Eye Res* **26**: 233–253.
22. Parry, HB (1953). Degenerations of the dog retina. II. Generalized progressive atrophy of hereditary origin. *Br J Ophthalmol* **37**: 487–502.
23. Petit, L, Lhériteau, E, Weber, M, Le Meur, G, Deschamps, JY, Provost, N *et al.* (2012). Restoration of vision in the pde6β-deficient dog, a large animal model of rod-cone dystrophy. *Mol Ther* **20**: 2019–2030.
24. Szél, A, Röhlich, P, Caffé, AR and van Veen, T (1996). Distribution of cone photoreceptors in the mammalian retina. *Microsc Res Tech* **35**: 445–462.
25. Szél, A, Röhlich, P, Mieziewska, K, Aguirre, G and van Veen, T (1993). Spatial and temporal differences between the expression of short- and middle-wave sensitive cone pigments in the mouse retina: a developmental study. *J Comp Neurol* **331**: 564–577.
26. Ortín-Martínez, A, Jiménez-López, M, Nadal-Nicolás, FM, Salinas-Navarro, M, Alarcón-Martínez, L, Sauvé, Y *et al.* (2010). Automated quantification and topographical distribution of the whole population of S- and L-cones in adult albino and pigmented rats. *Invest Ophthalmol Vis Sci* **51**: 3171–3183.
27. Kim, C, Kim, KJ, Bok, J, Lee, EJ, Kim, DJ, Oh, JH *et al.* (2012). Microarray-based mutation detection and phenotypic characterization in Korean patients with retinitis pigmentosa. *Mol Vis* **18**: 2398–2410.

28. Lin, B, Masland, RH and Strettoi, E (2009). Remodeling of cone photoreceptor cells after rod degeneration in rd mice. *Exp Eye Res* **88**: 589–599.
29. Milam, AH, Li, ZY and Fariss, RN (1998). Histopathology of the human retina in retinitis pigmentosa. *Prog Retin Eye Res* **17**: 175–205.
30. Jacobson, SG, Roman, AJ, Aleman, TS, Sumaroka, A, Herrera, W, Windsor, EA *et al.* (2010). Normal central retinal function and structure preserved in retinitis pigmentosa. *Invest Ophthalmol Vis Sci* **51**: 1079–1085.
31. Aït-Ali, N, Fridlich, R, Millet-Puel, G, Clérin, E, Delalande, F, Jaillard, C *et al.* (2015). Rod-derived cone viability factor promotes cone survival by stimulating aerobic glycolysis. *Cell* **161**: 817–832.
32. Punzo, C, Kornacker, K and Cepko, CL (2009). Stimulation of the insulin/mTOR pathway delays cone death in a mouse model of retinitis pigmentosa. *Nat Neurosci* **12**: 44–52.
33. Mohand-Said, S, Deudon-Combe, A, Hicks, D, Simonutti, M, Forster, V, Fintz, AC *et al.* (1998). Normal retina releases a diffusible factor stimulating cone survival in the retinal degeneration mouse. *Proc Natl Acad Sci USA* **95**: 8357–8362.
34. Komeima, K, Rogers, BS and Campochiaro, PA (2007). Antioxidants slow photoreceptor cell death in mouse models of retinitis pigmentosa. *J Cell Physiol* **213**: 809–815.
35. Cideciyan, AV, Jacobson, SG, Beltran, WA, Sumaroka, A, Swider, M, Iwabe, S *et al.* (2013). Human retinal gene therapy for Leber congenital amaurosis shows advancing retinal degeneration despite enduring visual improvement. *Proc Natl Acad Sci USA* **110**: E517–E525.
36. Mowat, FM, Breuwer, AR, Bartoe, JT, Annear, MJ, Zhang, Z, Smith, AJ *et al.* (2013). RPE65 gene therapy slows cone loss in Rpe65-deficient dogs. *Gene Ther* **20**: 545–555.
37. Acland, GM, Aguirre, GD, Ray, J, Zhang, Q, Aleman, TS, Cideciyan, AV *et al.* (2001). Gene therapy restores vision in a canine model of childhood blindness. *Nat Genet* **28**: 92–95.
38. Narfström, K, Katz, ML, Ford, M, Redmond, TM, Rakoczy, E and Bragadóttir, R (2003). *In vivo* gene therapy in young and adult RPE65-/- dogs produces long-term visual improvement. *J Hered* **94**: 31–37.
39. Rolling, F, Le Meur, G, Stieger, K, Smith, AJ, Weber, M, Deschamps, JY *et al.* (2006). Gene therapeutic prospects in early onset of severe retinal dystrophy: restoration of vision in RPE65 Briard dogs using an AAV serotype 4 vector that specifically targets the retinal pigmented epithelium. *Bull Mem Acad R Med Belg* **161**: 497–508; discussion 508.
40. Jacobson, SG, Cideciyan, AV, Roman, AJ, Sumaroka, A, Schwartz, SB, Heon, E *et al.* (2015). Improvement and decline in vision with gene therapy in childhood blindness. *N Engl J Med* **372**: 1920–1926.
41. Bainbridge, JW, Mehat, MS, Sundaram, V, Robbie, SJ, Barker, SE, Ripamonti, C *et al.* (2015). Long-term effect of gene therapy on Leber's congenital amaurosis. *N Engl J Med* **372**: 1887–1897.
42. Koch, SF, Tsai, YT, Duong, JK, Wu, WH, Hsu, CW, Wu, WP *et al.* (2015). Halting progressive neurodegeneration in advanced retinitis pigmentosa. *J Clin Invest* **125**: 3704–3713.
43. Narfström, K, Ekesten, B, Rosolen, SG, Spiess, BM, Percicot, CL and Ofri, R; Committee for a Harmonized ERG Protocol, European College of Veterinary Ophthalmology (2002). Guidelines for clinical electroretinography in the dog. *Doc Ophthalmol* **105**: 83–92.
44. Lhériteau, E, Libeau, L, Mendes-Madeira, A, Deschamps, JY, Weber, M, Le Meur, G *et al.* (2010). Regulation of retinal function but nonrescue of vision in RPE65-deficient dogs treated with doxycycline-regulatable AAV vectors. *Mol Ther* **18**: 1085–1093.